proceedings

Proceedings

Exergy Analysis of Waste Incineration Plant: Flue Gas reCirculation and Process Optimization †

Giorgio Vilardi * and Nicola Verdone

Department of Chemical Engineering Materials Environment, University of Rome La Sapienza, Via Eudossiana 18, 00184 Rome, Italy; nicola.verdone@uniroma1.it

* Correspondence: giorgio.vilardi@uniroma1.it

† Presented at the First World Energies Forum, 14 September–05 October 2020; Available online: https://wef.sciforum.net/.

Published: 12 September 2020

Abstract: Simulations of two incineration processes, with and without flue gas recirculation, have been carried out performing also an exergy analysis, to investigate on the most critical equipment unit in terms of second-law efficiency. Flue gas from the economizer outlet is employed to partially replace secondary combustion air, to reduce, at the same time, incinerator temperature and oxygen concentration. Conversely, in the proposed configuration the recirculated flue gas flow rate is used to control incinerator temperature, while the air flow rate is used to control the oxygen content of the fumes leaving the incinerator to be as close to 6% as possible, i.e., the minimum allowed for existing plants to ensure completion of the combustion reactions, and determines the corresponding minimum flue gas flow rate. The flue gas recirculation guarantees a larger level of energy recovery (up to +3%) and, at the same time, lower investment costs for the lower flow rate of fumes actually emitted if compared to the plant configuration without flue gas recirculation. Various operating parameters were varied (incinerator's effluent gas superheating temperature, air flowrate, oxygen % in air flowrate, flue gas recirculation flowrate) to investigate on their influence on process exergy efficiency. Exergy analysis allowed to individuate the equipment units characterized by larger exergy destruction and demonstrated that the flue gas recirculation led to an overall process exergy efficiency increase of about 3%.

Keywords: incineration; MSW; chemical-exergy

1. Introduction

The quick population growth and high raw materials consumption are leading to a substantial increase of the municipal solid waste (MSW) produced worldwide, which has a remarkable negative impact on life quality [1]. MSW incineration, among other possible waste treatment processes, represented a well-known technology, that can also allow to transform waste into mechanical power, according to the waste to energy (WtE) approach [2]. WtE can be considered an important choice for waste management: indeed, in 2015 about 2200 waste incineration plants were operative worldwide, with a capacity of 280 Mt/d [3]. It has been estimated that a reduction of 10–15% of GHG emissions can be reached by improving MSW management [4]. Although the notable advantages of MSW incineration, some disadvantages still reduced the overall efficiency and limited the environmental benefits of this process: by-products production (bottom and fly ashes, on which intensive research on their reuse is currently going on [5]), combustion instabilities, toxic gaseous pollutants and heavy metals emissions [6]. In this framework, exergy analysis may be a fundamental tool to individuate thermodynamic irreversibility and waste streams basing on second principle, overcoming the drawbacks of first principle analysis of existing and new power plants.

The present work reports the exergy analysis of a previous simulated incineration plant, integrated with steam and work production cycle but without considering the flue gas treatment system [7].

2. Materials and Methods

The process was built in PRO/II simulation environment (see Figure 1).

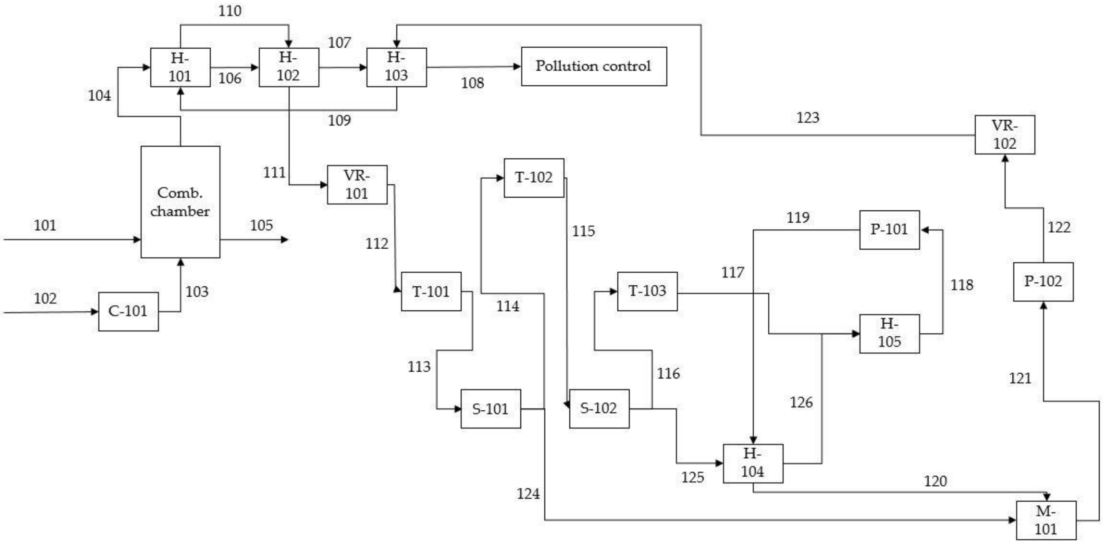

Figure 1. MSW incineration plant scheme without FGR.

The MSW (101) enters the incinerator with air compressed with a blower (C-101) up to 1.04 bar (103), then the flue gas (104) is sent to the boiler, represented by three heat exchangers (H-101 the vaporizer, H-102 the superheater and H-103 the economizer), the produced steam is then sent to the turbines for the work generation by steam expansion. Then, the obtained condensed water is recirculated (by the pump P-102). The exhaust gas (108) is sent to the treatment units. The temperature of the flue gas and the oxygen %mol (kept >6% on wet basis, according to current legislation [7]) were controlled by manipulating air inlet flowrate and flue gas recirculation. The equipment has been indicated as follows: C-Compressor, P-Pump, S-Splitter, M-Mixer, H-Heat Exchanger, T-Turbine and VR-Regulator valve.

The exhaust gas treatment section aimed to reduce HCl and SO_2 concentration to the EC regulation (Directive 2010/75/EU) and their modelling was limited to the pressure drop and power of the pump estimation for energy and exergy analysis. The temperature of stream 108, exhaust gas exiting from the boiler, was set equal to 200°C basing on the actual trend for energy efficiency increase. The thermal input was 22 MW (8.28 t/h of MSW), whereas the heat loss from the incinerator as radiative heat loss was 0.93 MW. More details are reported in Liuzzo et al., 2007 [7]. The MSW characteristics (proximate and ultimate analysis) are reported in Table 1.

Table 1. MSW characteristics (from [7]).

MSW Analysis	U.M.	Value
Moisture	%wt	25.2
Ash	%wt	24.4
Fixed carbon and volatile matter	%wt	50.4
C	%wt	50.8
H	%wt	6.8
O	%wt	40.3
N	%wt	1
Cl	%wt	0.8
S	%wt	0.3
LHV *	kJ/kg	9570

* LHV is the lower heating value.

The same overall process was simulated adopting flue gas recirculation (FGR) (see Figure 2).

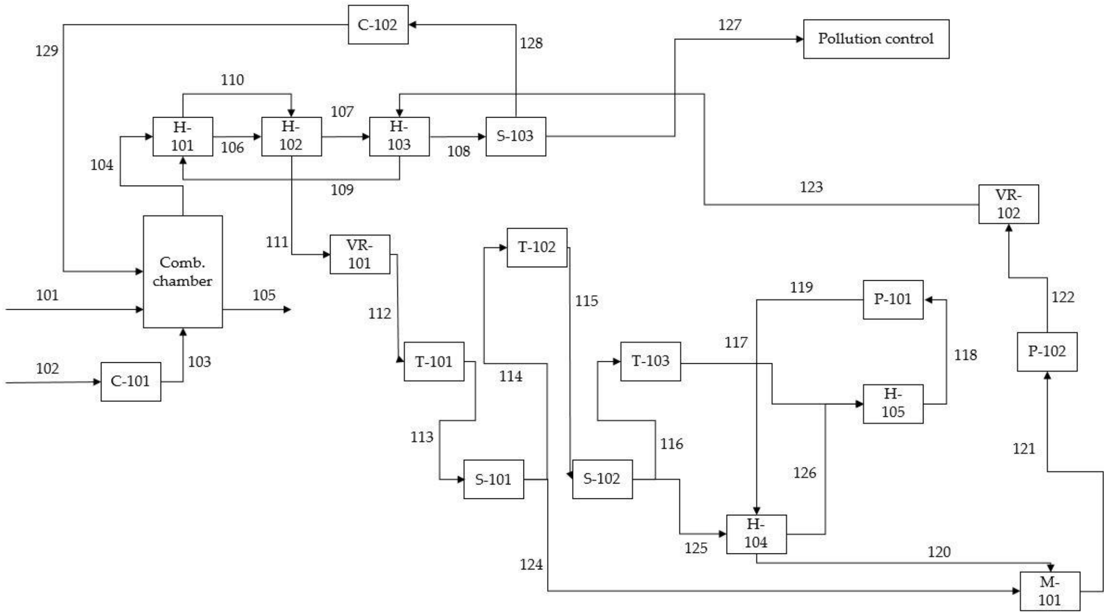

Figure 2. MSW incineration plant scheme with FGR.

The simulations were carried out at two different temperature of the combustion chamber, i.e., the temperature of exiting flue gas (950 and 1100 °C) and the operative conditions and assumptions related to the other plant units are reported in Table 2 (ΔP [bar] represents pressure drop term).

Table 2. Equipment characteristic parameters (from [7]).

Plant Unit Parameter	U.M.	Value
Turbine adiabatic efficiency	%	84
Losses at turbine discharge	bar	0.056
Pumps and blowers efficiency	%	70
ΔP boiler water side	bar	3.04
ΔP boiler fumes side	bar	0.05
Discharge head of P-102	bar	47.62
ΔP VR-101	bar	2.03
ΔP VR-103	bar	2.03
Steam pressure at condenser	bar	0.078
Superheated steam temperature	°C	360

As reported in Table 3, in this case, various benefits have been achieved, such as larger net overall efficiency (defined as the multiplication of boiler efficiency and the efficiency of thermal energy conversion into electric energy), lower inlet air flowrate and flue gas flowrate to the stack after its treatment (i.e., lower investment and operative costs of treatment units).

Table 3. Simulation results (from [7]).

Parameter	U.M.				
Temperature	**°C**	**950**		**1100**	
Air	kg/h	64,675	40,567	53,073	40,563
FGR	kg/h	-	26,761	-	13,376
Flue gas (to treatment)	kg/h	72,356	48,163	60,538	48,159
Net overall efficiency	%	21.7	23.5	22.8	23.7

For each equipment and for the overall process the physical and chemical exergy fluxes (in/out streams) have been calculated by the following equations [8]:

$$Ex_{in/out}^{ph} = M_{in/out}[(H - H_0) - T_0(S - S_0)] \quad (1)$$

$$Ex_{in/out}^{ch} = M_{in/out}\left(\sum_i^n x_i ex_i^{ch} + RT_0 \sum_i^n x_i \ln(x_i)\right) \quad (2)$$

where Ex_{in}^{ph} [kJ/h or kW] is the inlet/outlet physical exergy, M [kmol/h] is the molar flowrate of the considered stream, H [kJ/kmol] is the molar enthalpy of the stream at its P and T, H_0 [kJ/kmol] is the molar enthalpy of the stream at P = 1 atm and $T = T_0$ = 25 °C, i.e., the pressure and temperature of the dead state, S [kJ/K·kmol] is the entropy of the stream at its P and T and S_0 [kJ/K·kmol] is the entropy of the stream at dead state conditions [8], Ex_{in}^{ch} [kJ/h or kW] is the inlet/outlet chemical exergy, n is the number of chemical species, x_i is the mole fraction of i species, ex_i^{ch} (kJ/kmol) is the standard chemical exergy of i species at P = 1 atm and T_0 = 25 °C taken from [9,10] or calculated with the procedure reported by Gharagheizi and co-workers [9], R [kJ/K·kmol] is the gas constant.

In the calculations the kinetic and potential exergy are usually neglected since their order of magnitude is lower with respect to those of chemical and physical exergy contributions, therefore the exergy efficiency and destroyed exergy have been calculated as:

$$\eta = \frac{Ex_{prod}^{tot}}{Ex_{feed}^{tot}} = 1 - \frac{Ex_d^{tot}}{Ex_{feed}^{tot}} \quad (3)$$

$$Ex_d^{tot} = Ex_{feed}^{tot} - Ex_{prod}^{tot} = T_0 S_{gen} \quad (4)$$

where Ex^{tot}_{prod} and Ex^{tot}_{feed} are the total exergy produced from the system and fed to the system, respectively and S_{gen} [kJ/K·kmol] is the entropy generated.

3. Results

3.1. Exergy Analysis Results without FGR

Tables 4–7 summarize the results obtained at 950 °C and 1100 °C.

Table 4. Equipment exergy analysis results at 950°C.

Unit	Exergy Produced (kW)	Exergy Feed (kW)	Irreversibility (kW)	Waste (kW)	η
C-101	Ex,103–Ex,102 55.07	Ex,C-101 78	22.93	0	0.706
P-101	Ex,119–Ex,118 2.53	Ex,P-101 3.00	0.47	0	0.842
P-102	Ex,122–Ex,121 39.56	Ex,P-102 46	10.89	0	0.768
T-101	Ex,T-101 −3058	Ex,112–Ex,113 3639	580.89	0	0.84
T-102	Ex,T-102 −963	Ex,114–Ex,115 1147	184.22	0	0.837
T-103	Ex,T-103 −1681	Ex,116–Ex,117 2056	374.56	0	0.818
H-101	Ex,110–Ex,109 4988.89	Ex,104–Ex,106 8044	3055.56	0	0.620
H-102	Ex,111–Ex,110 1261	Ex,106–Ex,107 1472.22	211.11	0	0.857
H-103	Ex,109–Ex,123 1972.22	Ex,107–Ex,108 1994.44	22.22	0	0.989
H-104	Ex,120–Ex,119 338.85	Ex,125–Ex,126 352.42	13.57	0	0.961
H-105	Ex,q,H-105 723.12	Ex,126+Ex,117-Ex,118 1422.29	699.17	0	0.508
C.Chamber	Ex,104 13,359.15	Ex,101+Ex,103 19,051.43	5692.18	Ex,Ash 0.09	0.701

Table 5. Cycle exergy analysis results at 950 °C.

Exergy Produced (kW)	Exergy Feed (kW)	Irreversibility (kW)	Waste (kW)	η
Ex,T-101+Ex,T-102+Ex,T-103+Ex,q,H-105 5702.00	Ex,101+Ex,102+Ex,P-101+Ex,P-102+Ex,C-101 18,401	10,851	Ex,108+Ex,Ash 1848	0.31

Table 6. Equipment exergy analysis results at 1100°C.

Unit	Exergy Produced (kW)	Exergy Feed (kW)	Irreversibility (kW)	Waste (kW)	η
C-101	Ex,103–Ex,102 45.21	Ex,C-101 64	18.79	0	0.706
P-101	Ex,119–Ex,118 2.58	Ex,P-101 3.00	0.42	0	0.860
P-102	Ex,122–Ex,121 39.56	Ex,P-102 46	11.89	0	0.752
T-101	Ex,T-101 −3123	Ex,112-Ex,113 3717	593.67	0	0.84
T-102	Ex,T-102 −983	Ex,114-Ex,115 1169	186.44	0	0.837
T-103	Ex,T-103 −1717	Ex,116–Ex,117 2100	383.00	0	0.818
H-101	Ex,110–Ex,109 5088.89	Ex,104–Ex,106 8078	2988.89	0	0.630
H-102	Ex,111–Ex,110 1300	Ex,106–Ex,107 1613.89	313.89	0	0.806
H-103	Ex,109–Ex,123 1972.22	Ex,107–Ex,108 2147.22	175.00	0	0.918
H-104	Ex,120–Ex,119 345.71	Ex,125–Ex,126 360.45	14.75	0	0.959
H-105	Ex,q,H-105 738.50	Ex,126+Ex,117-Ex,118 1451.72	713.22	0	0.509
C.Chamber	Ex,104 13,734.58	Ex,101+Ex,103 19,026.63	5291.96	Ex,Ash 0.09	0.722

Table 7. Cycle exergy analysis results at 1100 °C.

Exergy Produced (kW)	Exergy Feed (kW)	Irreversibility (kW)	Waste (kW)	η
Ex,T-101+Ex,T-102+Ex,T-103+Ex,q,H-105 5823.00	Ex,101+Ex,102+Ex,P-101+Ex,P-102+Ex,C-101 18,373	10,702	Ex,108+Ex,Ash 1848	0.32

3.2. Exergy Analysis Results with FGR

Tables 8–11 summarize the results obtained at 950 °C and 1100 °C.

Table 8. Equipment exergy analysis results at 950 °C.

Unit	Exergy Produced (kW)	Exergy Feed (kW)	Irreversibility (kW)	Waste (kW)	η
C-101	Ex,103–Ex,102 34.52	Ex,C-101 49	14.48	0	0.705
C-102	Ex,129–Ex,128 119.44	Ex,C-102 146.00	26.56	0	0.818
P-101	Ex,119–Ex,118 2.69	Ex,P-101 3.00	0.31	0	0.896
P-102	Ex,122–Ex,121 39.56	Ex,P-102 46	5.56	0	0.889
T-101	Ex,T-101 −3253	Ex,112–Ex,113 3858	605.33	0	0.843
T-102	Ex,T-102 −1024	Ex,114–Ex,115 5367	4342.67	0	0.837
T-103	Ex,T-103 −1789	Ex,116–Ex,117 2186	397.11	0	0.818

H-101	Ex,110–Ex,109 5443.49	Ex,104–Ex,106 8539	3095.39	0	0.637
H-102	Ex,111–Ex,110 1206	Ex,106–Ex,107 1616.67	411.11	0	0.746
H-103	Ex,109–Ex,123 2102.78	Ex,107–Ex,108 2171.39	68.61	0	0.968
H-104	Ex,120–Ex,119 359.42	Ex,125–Ex,126 376.51	17.10	0	0.955
H-105	Ex,q,H-105 769.28	Ex,126+Ex,117-Ex,118 1513.37	744.09	0	0.508
C.Chamber	Ex,104 15,279.16	Ex,101+Ex,103+Ex,129 20,173.35	4894.10	Ex,Ash 0.09	0.757

Table 9. Cycle exergy analysis results at 950°C.

Exergy Produced (kW)	**Exergy Feed (kW)**	**Irreversibility** (kW)	**Waste (kW)**	***η***
Ex,T-101+Ex,T-102+Ex,T-103+Ex,q,H-105 6266.00	Ex,101+Ex,102+Ex,P-101+Ex,P-102+Ex,C-101+Ex,C-102 18,444	10,478	Ex,127+Ex,Ash 1900	0.340

Table 10. Equipment exergy analysis results at 1100°C.

Unit	**Exergy Produced (kW)**	**Exergy Feed (kW)**	**Irreversibility (kW)**	**Waste (kW)**	***η***
C-101	Ex,103–Ex,102 34.11	Ex,C-101 49	14.89	0	0.696
C-102	Ex,129–Ex,128 30.45	Ex,C-102 38.00	7.55	0	0.801
P-101	Ex,119–Ex,118 2.69	Ex,P-101 3.00	0.31	0	0.896
P-102	Ex,122–Ex,121 39.56	Ex,P-102 46	5.56	0	0.889
T-101	Ex,T-101 −3253	Ex,112-Ex,113 3858	605.33	0	0.843
T-102	Ex,T-102 −1024	Ex,114–Ex,115 5367	4342.67	0	0.837
T-103	Ex,T-103 −1789	Ex,116–Ex,117 2186	397.11	0	0.818
H-101	Ex,110–Ex,109 5443.49	Ex,104–Ex,106 9083	3639.84	0	0.599
H-102	Ex,111–Ex,110 1206	Ex,106–Ex,107 1722.22	516.67	0	0.700
H-103	Ex,109–Ex,123 2102.78	Ex,107–Ex,108 2258.33	155.56	0	0.931
H-104	Ex,120–Ex,119 359.42	Ex,125–Ex,126 376.51	17.10	0	0.955
H-105	Ex,q,H-105 769.28	Ex,126+Ex,117-Ex,118 1513.37	744.09	0	0.508
C.Chamber	Ex,104 15,209.08	Ex,101+Ex,103+Ex,129 19,303.27	4094.10	Ex,Ash 0.09	0.788

Table 11. Cycle exergy analysis results at 1100°C.

Exergy Produced (kW)	**Exergy Feed (kW)**	**Irreversibility** (kW)	**Waste (kW)**	***η***
Ex,T-101+Ex,T-102+Ex,T-103+Ex,q,H-105	Ex,101+Ex,102+Ex,P-101+Ex,P-102+Ex,C-101+Ex,C-102	10,398	Ex,127+Ex,Ash	0.344
6311.00	18,335		1872	

4. Discussion

Besides H-105, the exergy efficiency of machinery and heat exchangers was always higher than 60% and the loss of exergy was due only to the irreversibility of the process (compression/heating, etc.). The H-105 was characterized by lower exergy efficiency because the heat transfer occurred with two mixed fluids entering the unit, streams 117 and 126, where stream 117 was characterized by a pressure of 0.081 bar and a low physical exergy with respect to that of streams 126 and outlet stream 118. Furthermore, the chemical exergy of stream 117 was one order of magnitude higher than that of stream 118. Due to the high chemical exergy of MSW in comparison with that of flue gas produced, the exergy efficiency of the combustion chamber was lower than 80%, even when FGR was adopted. FGR demonstrated to lead also to exergy efficiency improvement, besides the well-known environmental and economic benefits. The FGR allowed to increase η of 3% at 950 °C and about 2.5% at 1100 °C. The increase of temperature in combustion chamber led also to exergy efficiency improvement, because of the larger power produced by the three turbines with respect to the exergy feed flow, and, therefore, lower irreversibility and waste. The FGR allowed to reduce exergy loss as waste, since an aliquot of FGR will be recirculated and will not be sent to pollution treatment units. The second configuration required an additional compressor (C-102) but the FGR adoption permitted to reduce the power consumption of the first compressor unit because of the lower oxidant inlet flowrate and lower exergy feed flow.

Funding: This research received no external funding.

Conflicts of Interest: The authors declare no conflict of interest.

References

1. Blasenbauer, D.; Huber, F.; Lederer, J.; Quina, M.J.; Blanc-Biscarat, D.; Bogush, A.; Bontempi, E.; Blondeau, J.; Chimenos, J.M.; Dahlbo, H.; et al. Legal situation and current practice of waste incineration bottom ash utilisation in Europe. *Waste Manag.* **2020**, *102*, 868–883, doi:10.1016/j.wasman.2019.11.031.
2. Wu, Y.; Tao, Y.; Deng, Z.; Zhou, J.; Xu, C.; Zhang, B. A fuzzy analysis framework for waste incineration power plant comprehensive benefit evaluation from refuse classification perspective. *J. Clean. Prod.* **2020**, *258*, 120734, doi:10.1016/j.jclepro.2020.120734.
3. Wissing, F.; Wirtz, S.; Scherer, V. Simulating municipal solid waste incineration with a DEM/CFD method—Influences of waste properties, grate and furnace design. *Fuel.* **2017**, *206*, 638–656, doi:10.1016/j.fuel.2017.06.037.
4. Scarlat, N.; Fahl, F.; Dallemand, J.F. Status and Opportunities for Energy Recovery from Municipal Solid Waste in Europe. *Waste Biomass Valorization* **2019**, *10*, 2425–2444, doi:10.1007/s12649-018-0297-7.
5. Cristelo, N.; Segadães, L.; Coelho, J.; Chaves, B.; Sousa, N.R.; Lopes, M.d. Recycling municipal solid waste incineration slag and fly ash as precursors in low-range alkaline cements. *Waste Manag.* **2020**, *104*, 60–73, doi:10.1016/j.wasman.2020.01.013.
6. Ding, G.; He, B.; Cao, Y.; Wang, C.; Su, L.; Duan, Z.; Song, J.; Tong, W.; Li, X. Process simulation and optimization of municipal solid waste fired power plant with oxygen/carbon dioxide combustion for near zero carbon dioxide emission. *Energy Convers. Manag.* **2018**, *157*, 157–168, doi:10.1016/j.enconman.2017.11.087.
7. Liuzzo, G.; Verdone, N.; Bravi, M. The benefits of flue gas recirculation in waste incineration. *Waste Manag.* **2007**, *27*, 106–116, doi:10.1016/j.wasman.2006.01.002.
8. Kotas, T.J. *The Exergy Method of Thermal Plant Analysis*; Elsevier: London, UK, 1985, doi:10.1016/C2013-0-00894-8.

9. Gharagheizi, F.; Ilani-Kashkouli, P.; Hedden, R.C. Standard molar chemical exergy: A new accurate model. *Energy* **2018**, *158*, 924–935, doi:10.1016/J.ENERGY.2018.05.186.
10. Morris, D.R.; Szargut, J. Standard chemical exergy of some elements and compounds on the planet earth. *Energy* **1986**, *11*, 733–755, doi:10.1016/0360-5442(86)90013-7.